

Camera-based Pulse-Oximetry - Validated Risks and Opportunities from Theoretical Analysis

MARK VAN GASTEL,^{1,*} SANDER STUIJK,¹ AND GERARD DE HAAN^{1,2}

¹Department of Electrical Engineering, Eindhoven University of Technology, PO Box 513, 5600MB, Eindhoven, The Netherlands

²Philips Research, High Tech Campus 34, 5656AE, Eindhoven, The Netherlands

*m.j.h.v.gastel@tue.nl

Abstract: Camera-based pulse-oximetry has recently shown to be feasible, even when the signal is corrupted by noise and motion artifacts. Earlier work showed that using three instead of the common two wavelengths improves robustness of the measurement, however without a thorough investigation on the optimal wavelength selection. We therefore performed a search to identify these wavelengths to further improve the robustness of the measurement. Besides motion, it is empirically known that there are several other factors that influence the measurement leading to falsely-low or falsely-high SpO₂ readings. These factors include the presence of dyshemoglobins or other species. In this paper, we use a theoretical skin-model to study how these factors influence the measurement, and how a proper wavelength selection can reduce the impact on the measurement. Additionally, we show that adding a third wavelength does not only improve robustness, but can also be exploited to create a reliability index for the measurement. Finally, we show that the presence of dyshemoglobins in arterial blood can not only be detected but also quantified. We illustrate this by comparing the estimated COHb levels of a small group of smokers and non-smokers, which typically have different CO-levels.

© 2017 Optical Society of America

OCIS codes: (170.0170) Medical optics and biotechnology imaging system; (170.1470) Blood or tissue constituent monitoring; (280.0280) Remote sensing and sensors; (170.3660) Light propagation in tissues

References and links

1. T. Aoyagi, M. Kishi, K. Yamaguchi, and S. Watanabe, "Improvement of the earpiece oximeter," Japanese Society of Medical Electronics and Biological Engineering, 90–91 (1974).
2. W. Verkruysse, M. Bartula, E. Bresch, M. Rocque, M. Meftah, and I. Kirenko, "Calibration of contactless pulse oximetry," *Anesth. Analg.* **124**(1), 136 (2017).
3. M. van Gastel, S. Stuijk, and G. de Haan, "New principle for measuring arterial blood oxygenation, enabling motion-robust remote monitoring," *Sci. Rep.* **6**, 38609 (2016).
4. R. Miller, L. Eriksson, L. Fleisher, J. Wiener-Kronish, and W. Young, *Anesthesia* (Elsevier Health Sciences, 2009).
5. S. J. Barker and K. K. Tremper, "The effect of carbon monoxide inhalation on pulse oximetry and transcutaneous PO₂," *Anesthesiology* **66**(5), 677–679 (1987).
6. S. Barker and J. Badal, "The measurement of dyshemoglobins and total hemoglobin by pulse oximetry," *Current Opinion in Anesthesiology* **21**(6), 805–810 (2008).
7. S. Barker, K. Tremper, and J. Hyatt, "Effects of methemoglobinemia on pulse oximetry and mixed venous oximetry," *Anesthesiology* **70**(1), 112–117 (1989).
8. G. Clarke, A. Chan, and A. Adler, "Effects of motion artifact on the blood oxygen saturation estimate in pulse oximetry," in *Medical Measurements and Applications (MeMeA), 2014 IEEE International Symposium on*, (IEEE, 2014), pp. 1–4.
9. T. Jensen, S. Duun, J. Larsen, R. Haahr, M. Toft, B. Belhage, and E. Thomsen, "Independent component analysis applied to pulse oximetry in the estimation of the arterial oxygen saturation (SpO₂)-a comparative study," in *Engineering in Medicine and Biology Society, 2009. Annual International Conference of the IEEE*, (IEEE, 2009), pp. 4039–4044.
10. M. Ram, K. Madhav, E. Krishna, N. Komalla, and K. Reddy, "A novel approach for motion artifact reduction in ppg signals based on as-lms adaptive filter," *IEEE Trans. Instrum. Meas.* **61**(5), 1445–1457 (2012).
11. E. Chan, M. Chan, and M. Chan, "Pulse oximetry: understanding its basic principles facilitates appreciation of its limitations," *Respir. Med.* **107**(6), 789–799 (2013).
12. C. Secker and P. Spiers, "Accuracy of pulse oximetry in patients with low systemic vascular resistance," *Anaesthesia* **52**(2), 127–130 (1997).
13. B. Wilson, H. Cowan, J. Lord, D. Zuege, and D. Zygun, "The accuracy of pulse oximetry in emergency department patients with severe sepsis and septic shock: a retrospective cohort study," *BMC Emerg. Med.* **10**(1), 9 (2010).

14. A. A. Kamshilin, E. Nippolainen, I. S. Sidorov, P. V. Vasilev, N. P. Erofeev, N. P. Podolian, and R. V. Romashko, "A new look at the essence of the imaging photoplethysmography," *Sci. Rep.* **5**, 10494 (2015).
15. M. V. Volkov, N. B. Margaryants, A. V. Potemkin, M. A. Volynsky, I. P. Gurov, O. V. Mamontov, and A. A. Kamshilin, "Video capillaroscopy clarifies mechanism of the photoplethysmographic waveform appearance," *Sci. Rep.* **7**, 13298 (2017).
16. J. L. Reuss and D. Siker, "The pulse in reflectance pulse oximetry: modeling and experimental studies," *J. Clin. Monit. Comput.* **18**(4), 289–299 (2004).
17. J. L. Reuss, "Multilayer modeling of reflectance pulse oximetry," *IEEE Trans. Biomed. Eng.* **52**(2), 153–159 (2005).
18. M. Marshall, S. Kales, D. Christiani, and R. Goldman, "Are reference intervals for carboxyhemoglobin appropriate? A survey of Boston area laboratories," *Clin. Chem.* **41**(10), 1434–1438 (1995).
19. W. Zijlstra, A. Buursma, and W. Meeuwse-Van der Roest, "Absorption spectra of human fetal and adult oxyhemoglobin, de-oxyhemoglobin, carboxyhemoglobin, and methemoglobin," *Clin. Chem.* **37**(9), 1633–1638 (1991).
20. V. Rajadurai, A. Walker, V. Yu, and A. Oates, "Effect of fetal haemoglobin on the accuracy of pulse oximetry in preterm infants," *J. Paediatr. Child Health* **28**(1), 43–46 (1992).
21. P. Cornelissen, C. van Woensel, W. Van Oel, and P. De Jong, "Correction factors for hemoglobin derivatives in fetal blood, as measured with the il 282 co-oximeter," *Clin. Chem.* **29**(8), 1555–1556 (1983).

1. Introduction

Blood transports oxygen from the lungs to the various tissue cells of the human body. Hemoglobin (Hb) is the oxygen-binding protein contained in red blood cells (erythrocytes). In a healthy human the arterial hemoglobin is nearly saturated with oxygen (100% HbO₂, 0% Hb). In the past, arterial blood oxygenation was determined by analysing blood samples drawn from the arteries. Since its introduction in the early 1970s [1], pulse-oximetry has rapidly gained popularity as a non-invasive alternative for measurement of blood oxygenation levels. Essentially, pulse-oximetry optically monitors arterial oxygenation, using absorption differences between Hb and HbO₂. To differentiate between the readings of the invasive method involving blood gas analysis and the non-invasive optical method, oxygen saturation readings using the latter method are denoted with SpO₂, whereas the invasive measurements are denoted with SaO₂. Because of their low-cost, simplicity and non-invasiveness, pulse-oximeters have been quickly adopted, and are nowadays ubiquitously applied in clinical practise. More recently, contactless camera-based pulse-oximetry has shown promise of completely unobtrusive patient monitoring [2], which justified efforts to design a robust measurement principle [3]. Although the optical measurements generally correspond well with an invasive measurement, some realistic conditions can cause spurious readings. Particularly, dyshemoglobins with different absorption spectra shown in Fig. 1, but also

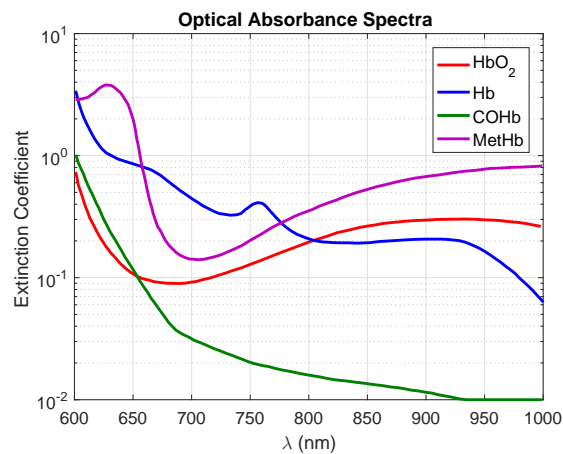


Fig. 1: Optical absorbance spectra of oxyhemoglobin (HbO₂), reduced hemoglobin (Hb), carboxyhemoglobin (COHb) and methemoglobin (MetHb) [4].

motion artifacts, and various physiological and pathological conditions can cause problems with optical measurements. When a hemoglobin molecule lost the capacity of reversibly binding oxygen under physiological conditions, either permanently or temporarily, it is denoted as a dyshemoglobin. The two most common variants of dyshemoglobin are carboxyhemoglobin (COHb) and methemoglobin (MetHb).

In this study, we investigate how these conditions affect the reading based on our developed opto-physiological models, the result of which we compare with empirical data from the literature. Next, we show how wavelength selection for camera-based pulse-oximetry can improve robustness and reduce the impact of some of the mentioned conditions on the SpO₂ measurement. We identify optimal wavelengths for these conditions together with their gains. Finally, we show that additional wavelength-channels enable the detection of unreliable readings, and the quantification of dyshemoglobin levels. An illustrative study for the quantification of a common dyshemoglobin in smokers, COHb, is included for a 3-wavelength camera.

2. Materials and Methods

In this section, we will first introduce the various sources of error in optical SpO₂-measurements. Next, in order to be able to quantify the effects of dyshemoglobin on the SpO₂ reading, we will introduce the calibration models required to relate the optical measurement to SpO₂ values, both for the common ‘ratio-of-ratios’ method [1] and for the recently introduced motion-robust ‘indirect’ APBV method [3]. These models assume the absence of other absorbers in pulsating arterial blood besides Hb and HbO₂. Thereafter we shall extend the calibration models to include the dyshemoglobins COHb and MetHb. The resulting models are Eq. (20), (22) and (23), which are a function of both oxygen saturation and dyshemoglobin concentration. Sections 2.2 and 2.3, present the derivation of the models and their verification using measured effects reported in the literature.

2.1. Sources of error

Because of the different absorption spectra and the inability of dual-wavelength pulse-oximeters to differentiate between more than two species, the presence of dyshemoglobins in arterial blood can cause spurious SpO₂ readings. For carboxyhemoglobin there is a linear decline in HbO₂ saturation reported as COHb saturation increases. This decline is not detected by pulse-oximetry, which therefore overestimates HbO₂ saturation in patients with increased COHb levels [5, 6]. Similarly, the significant effects of elevated levels of MetHb on the SpO₂ reading have been reported [6, 7]. For high concentrations, methemoglobin causes the SpO₂ reading to become approximately 85%, independent of the true oxygenation level.

Motion because of excessive movements for normal oxygenation levels could cause a falsely-low SpO₂ reading because of the corrupted measurements of the features extracted from the PPG waveforms [8]. Attempts have been made to isolate the cardiac pulse signal from other components present in the waveforms, e.g. by employing adaptive filters [9, 10]. Blood saturation during motion remains however challenging because of the many confounding factors during movements: venous pulsations, sensor-tissue motion and sensor deformation. Recently we showed that for the contactless camera-based approach the pulse signal can be isolated by exploiting the fact that motion affects the waveforms differently compared to the cardiac-induced blood volume variations [3], enabling motion-tolerant SpO₂ monitoring. Ballistocardiographic (BCG) motion is a special case of motion distortions, which in contrary to the excessive movements has a cardiac-similar frequency. Consequently, also applying advanced frequency-based methods to isolate the pulse signal would lead to a corrupted measurement because of this mixture of motion and blood volume variations. The presence of BCG artifacts is dependent on the measurement site and how severe this effect is for both the contact-based and contactless measurement is not

well-studied yet.

Besides the causes mentioned above, there are more factors which could render the SpO₂ reading inaccurate [11]. For many factors however it is debatable if they significantly affect the reading since contradictory results have been reported in literature. An example of such factor is sepsis or septic shock. A study performed by Secker and Spiers [12], where they compared 80 paired SpO₂ and SaO₂ readings in patients with septic shock, reported statistical significant underestimation of SaO₂ by 1.4%, a level which is however unlikely to be clinically important. By contrast, a study performed by Wilson [13] on 88 patients with severe sepsis and septic shock, showed that SpO₂ significantly *overestimates* SaO₂ by nearly 5% in those with hypoxemia. Other causes mentioned in literature include physiological conditions such as severe hyperbilirubinemia, anemia and sulfhemoglobinemia, but also others factors such as poor probe positioning or nail polish. In the remainder of this paper we will focus on the presence of motion artifacts and dyshemoglobins as the main causes of corrupted camera-based SpO₂ measurements.

The origin of the PPG signal is subject to debate recently for visible wavelengths [14, 15]. Experiments using green resulted in observations which contradicted the commonly accepted volumetric model. Although we will focus on wavelengths in red and near-infrared (NIR) with a much deeper skin penetration depth compared to blue and green, the interaction with capillary blood with a lower oxygenation level compared to arterial blood could potentially have an impact on our modelling. Based on validated Monte-Carlo simulations using a 6-layer skin model [16, 17], it was concluded that the PPG amplitudes for 660 and 890nm could be solely explained by displacement of non-blood tissue of the cutaneous plexus layer by the added arterial blood. A recent study on the feasibility of camera-based pulse-oximetry [2] showed that clinically accurate SpO₂ measurements using 675nm and 842nm are feasible. Under normoxic conditions, a decrease in ambient temperature from 23 to 7 degrees Celsius resulted in a calibration error of only 0.1%. We therefore expect the effects of light interaction with pulsatile capillary blood with a lower oxygenation level to be negligible for red and NIR wavelengths.

2.2. Calibration model

To relate optical measurements of blood volume variations to oxygenation levels, the light-tissue interaction has to be well-understood. The attenuation of light traveling through a uniform medium containing an absorbing substance can be described by Beer-Lambert's law:

$$I = I_0 e^{-A} = I_0 e^{-\epsilon(\lambda)cl}, \quad (1)$$

where I_0 is the intensity of the incident light, I is the light reflected from the skin and A denotes absorbance. The incident light decreases exponentially dependent on the wavelength-dependent extinction coefficient $\epsilon(\lambda)$, concentration of the absorbing medium c and the optical path length l . The skin can be modeled as a collection of N layers with different absorbing properties:

$$I = I_0 e^{-\sum_{i=1}^N \epsilon_i(\lambda)c_i l_i}. \quad (2)$$

The N absorbers can be merged and expressed as a quasi-static DC component and a time-varying, periodic AC component:

$$I = I_0 e^{-[\epsilon_{DC} c_{DC} l_{DC} + \epsilon_{AC} c_{AC} l_{AC}]}. \quad (3)$$

Here the DC component comprises, among others, the absorbance of melanin, tissue and venous blood. During the cardiac cycle the blood volume concentration in the arteries varies synchronous with the heart rate. At systole the blood volume in the arteries is maximum, whereas at the end of diastole the blood volume is at its minimum. Because of the difference in absorbing properties

between blood and tissue, this variation in blood concentration leads to a variation in reflected light captured by a photodiode or camera. By the definition of arterial blood oxygenation:

$$SaO_2 = \frac{c_{HbO_2}}{c_{Hb} + c_{HbO_2}} \times 100\%, \quad (4)$$

one would like to isolate and extract the term c_{AC} from Eq. (3), since this term consists of the mixture Hb and HbO₂ concentrations. The expression is however dependent on other unknown parameters which makes the problem ill-posed. Therefore some manipulations and assumptions have to be made. When filling in Eq. (3) for the systolic and diastolic phase of the cardiac cycle and taking the ratio of these expressions, one obtains:

$$\frac{I_s}{I_d} = \frac{I_{min}}{I_{max}} = \frac{I_0 e^{-\epsilon_{DC} c_{DC} l_{DC} - \epsilon_{AC} c_{AC} (l_a + \Delta l)}}{I_0 e^{-\epsilon_{DC} c_{DC} l_{DC} - \epsilon_{AC} c_{AC} l_a}} = \frac{I_0 e^{-\epsilon_{DC} c_{DC} l_{DC} - [\epsilon_{Hb} c_{Hb} + \epsilon_{HbO_2} c_{HbO_2}] (l_a + \Delta l)}}{I_0 e^{-\epsilon_{DC} c_{DC} l_{DC} - [\epsilon_{Hb} c_{Hb} + \epsilon_{HbO_2} c_{HbO_2}] l_a}}, \quad (5)$$

where l_a is the basal diameter of arterial vessel before pulsation and $l_a + \Delta l$ is the maximum variation of arterial diameter during pulsation. The square of arterial diameter is proportional to the blood concentration. When taking the natural logarithm of Eq. (5), the cardiac-synchronous change in absorbance (ΔA) can be expressed as:

$$\ln\left(\frac{I_s}{I_d}\right) = [\epsilon_{Hb} c_{Hb} + \epsilon_{HbO_2} c_{HbO_2}] \Delta l = \Delta A \approx \frac{AC}{DC}, \quad (6)$$

In this expression the emitted light intensity and all quasi-static DC components have been eliminated. The approximation with the AC over DC ratio holds since the pulsatile AC part of the PPG waveform is typically very small compared to the static DC part. We will perform the subsequent manipulations for the conventional ratio-of-ratios and APBV approaches separately to arrive at expressions applicable for SpO₂ measurements.

2.2.1. Ratio-of-ratios

When measuring the change in unscattered absorbance (Eq. (6)) at two distinct wavelengths, λ_1 and λ_2 , and taking the ratio of both expressions, one obtains:

$$R = \frac{\Delta A(\lambda_1)}{\Delta A(\lambda_2)} = \frac{A_{systole}(\lambda_1) - A_{diastole}(\lambda_1)}{A_{systole}(\lambda_2) - A_{diastole}(\lambda_2)} = \frac{[\epsilon_{Hb}(\lambda_1) c_{Hb} + \epsilon_{HbO_2}(\lambda_1) c_{HbO_2}] \Delta l_1}{[\epsilon_{Hb}(\lambda_2) c_{Hb} + \epsilon_{HbO_2}(\lambda_2) c_{HbO_2}] \Delta l_2}. \quad (7)$$

Here the ‘ratio-of-ratios’ R is still dependent on the unknown path length variations Δl . With the assumption that $\Delta l_1 \approx \Delta l_2$, this unknown parameter is eliminated. When substituting the definition of SaO₂, Eq. (4), into Eq. (7), R can be expressed as:

$$R = \frac{\epsilon_{Hb}(\lambda_1) + SaO_2 [\epsilon_{HbO_2}(\lambda_1) - \epsilon_{Hb}(\lambda_1)]}{\epsilon_{Hb}(\lambda_2) + SaO_2 [\epsilon_{HbO_2}(\lambda_2) - \epsilon_{Hb}(\lambda_2)]} = \frac{\ln\left(\frac{I_s}{I_d}\right)_{\lambda_1}}{\ln\left(\frac{I_s}{I_d}\right)_{\lambda_2}} \approx \frac{\left(\frac{AC}{DC}\right)_{\lambda_1}}{\left(\frac{AC}{DC}\right)_{\lambda_2}}. \quad (8)$$

When we for the moment assume SaO₂ and SpO₂ to be identical, SpO₂ can be expressed as a function of the ratio-of-ratios R, $SpO_2 = \alpha(R)$, and therefore applicable for optical blood oxygenation measurements:

$$SpO_2 = \frac{\epsilon_{Hb}(\lambda_1) - \epsilon_{Hb}(\lambda_2) R}{\epsilon_{Hb}(\lambda_1) - \epsilon_{HbO_2}(\lambda_1) + [\epsilon_{HbO_2}(\lambda_2) - \epsilon_{Hb}(\lambda_2)] R} \times 100\% \quad (9)$$

We are aware that in the optical model we make some assumptions which may not entirely reflect reality, e.g. we assume that the skin is homogeneous, scattering of light is not present and the

examined wavelengths are sampling the same depth. All these factors could impact the accuracy of the measurement. For these reasons, pulse-oximeters are usually calibrated empirically and not based on an optical model.

2.2.2. APBV

Instead of extracting features from the PPG waveforms, APBV determines SpO₂ indirectly based on the signal quality of the pulse signals extracted with SpO₂ ‘signatures’ [3]. This procedure can mathematically be described as:

$$SpO_2 = \underset{SpO_2 \in SpO_2}{\operatorname{argmax}} SNR \left(\overbrace{k \vec{P}_{bv}(SpO_2) [\mathbf{C}_n \mathbf{C}_n^T]^{-1} \mathbf{C}_n}^{\vec{W}_{PBV}} \right), \quad (10)$$

where \mathbf{C}_n contains the DC-normalized color variations and scalar k is chosen such that \vec{W}_{PBV} has unit length. The calculation of the weights for extraction of the pulse signal, \vec{W}_{PBV} , is formulated as a least squares problem using the SpO₂-dependent pulse prior \vec{P}_{bv} . The SpO₂ signatures compiled in \vec{P}_{bv} can be derived from physiology and optics. Assuming identical cameras the PPG amplitudes of N cameras can be determined by [3]:

$$\vec{P}_{bv} = \left\| \begin{bmatrix} \left(\frac{AC}{DC}\right)^1 \\ \left(\frac{AC}{DC}\right)^2 \\ \vdots \\ \left(\frac{AC}{DC}\right)^N \end{bmatrix} \right\| = \left\| \begin{bmatrix} \frac{\int_{\lambda} I(\lambda) F^1(\lambda) C(\lambda) PPG(\lambda) d\lambda}{\int_{\lambda} I(\lambda) F^1(\lambda) C(\lambda) \rho_s(\lambda) d\lambda} \\ \frac{\int_{\lambda} I(\lambda) F^2(\lambda) C(\lambda) PPG(\lambda) d\lambda}{\int_{\lambda} I(\lambda) F^2(\lambda) C(\lambda) \rho_s(\lambda) d\lambda} \\ \vdots \\ \frac{\int_{\lambda} I(\lambda) F^N(\lambda) C(\lambda) PPG(\lambda) d\lambda}{\int_{\lambda} I(\lambda) F^N(\lambda) C(\lambda) \rho_s(\lambda) d\lambda} \end{bmatrix} \right\|. \quad (11)$$

Here the PPG amplitude spectrum, $PPG(\lambda)$, can be approximated by a linear mixture of the light absorption spectra from the two most common variants of the main chromophore in arterial blood, hemoglobin; oxygenated (HbO₂) and reduced (Hb):

$$\begin{aligned} PPG(\lambda) &\approx \epsilon_{Hb}(\lambda) c_{Hb} + \epsilon_{HbO_2}(\lambda) c_{HbO_2} = (1 - SaO_2) \epsilon_{Hb}(\lambda) + SaO_2 \epsilon_{HbO_2}(\lambda) \\ &= \epsilon_{Hb}(\lambda) + SaO_2 [\epsilon_{HbO_2}(\lambda) - \epsilon_{Hb}(\lambda)], \end{aligned} \quad (12)$$

where we assume that the optical path length differences are negligible for $600 < \lambda < 1000\text{nm}$ and $SaO_2 \in [0, 1]$. We recognize that the wavelength-dependent effect of scattering could render this assumption invalid. The light spectrum, filter responses, camera sensitivity and skin reflectance are denoted with $I(\lambda)$, $F^i(\lambda)$, $C(\lambda)$, and $\rho_s(\lambda)$, in Eq. (11) respectively. By extracting the pulse signal for a collection of SpO₂ signatures over a range of oxygenation levels and measuring the signal quality of each signal, the pulse signal with the highest SNR value corresponds to the signature which describes the data best and therefore reflects the SpO₂ value. When using two wavelengths the ratio-of-ratios parameter R and the ratio of APBV parameter \vec{P}_{bv} , coincide. The wavelength selection of our previous publication [3] was based on three criteria: 1) the desire to measure oxygen saturation in darkness ($\lambda > 700\text{nm}$) for clinical applications, 2) have a reasonable SpO₂ contrast, and 3) wavelengths within the spectral sensitivity of the camera. Our decision to use three instead of the common two wavelengths used in pulse-oximetry was motivated by the improved robustness of the SpO₂ measurement by a factor of two. This can be explained by how motion affects the PPG waveforms when measured with a camera. Since motion-induced intensity variations are equal for all wavelengths, suppression of these artifacts is only possible for the APBV method if the pulse signature \vec{P}_{bv} is not equal to this motion signature, which can be described as a vector with equal weights. The SpO₂ calibration model

for the wavelengths used in [3] are visualized in Fig. 2. As can be observed from this figure, there does exist a motion-similar pulse signature when using two wavelengths, whereas there does not exist such a signature when adding a ‘redundant’ third wavelength enabling distinction between motion artifacts and the pulse signal for all oxygenation levels. Additionally, three wavelengths allow to suppress up to two independent (linear) noise sources, whereas two wavelengths can only eliminate one.

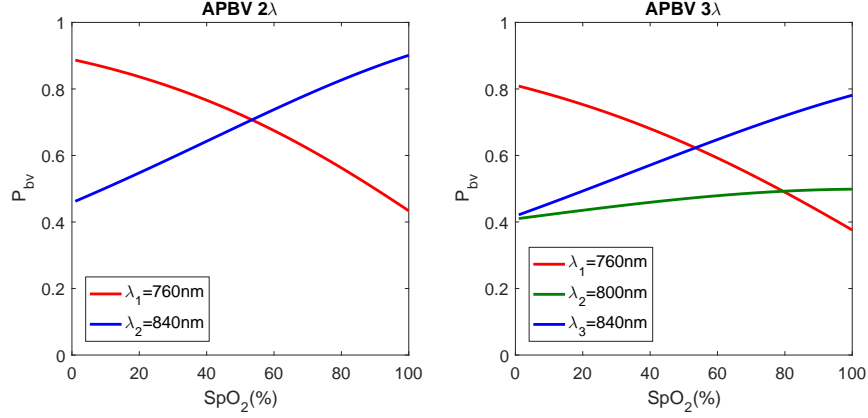


Fig. 2: Using three instead of two wavelengths for APBV improves robustness since motion affects all wavelengths equally. In contrast to the three wavelength calibration model (right), there does exist a motion-similar pulse signature when using two wavelengths, making it unable to distinguish between the pulse signal and motion.

2.3. Dyshemoglobins

The calibration models presented in the previous paragraph assume that Hb and HbO₂ are the only two absorbers in pulsatile arterial blood. To investigate how the addition of more absorbers influences calibration, we will extend the calibration models. After the introduction of the extended calibration model we will compare our results with the effects of dyshemoglobins reported in literature. First, we describe two definitions of arterial blood oxygenation, which are often misinterpreted in literature, leading to wrong conclusions. Functional hemoglobin saturation, $SaO_2^{functional}$, is defined as the ratio between HbO₂ and the sum of Hb and HbO₂:

$$SaO_2^{functional} = \frac{c_{HbO_2}}{c_{Hb} + c_{HbO_2}}. \quad (13)$$

The above definition of hemoglobin saturation is referred to as functional hemoglobin saturation because it ignores the two hemoglobin species which do not contribute to functional oxygen transport: carboxyhemoglobin and methemoglobin. When both dyshemoglobin species are taken into account, it is referred to as fractional hemoglobin saturation:

$$SaO_2^{fractional} = \frac{c_{HbO_2}}{c_{Hb} + c_{HbO_2} + c_{DysHb}} = \frac{c_{HbO_2}}{c_{Hb} + c_{HbO_2} + c_{COHb} + c_{MetHb}}. \quad (14)$$

Let us now introduce variable χ_i , which is defined as the *relative* concentration of chromophore i in pulsatile arterial blood:

$$\chi_i = \frac{C_i}{\sum_{i=1}^N C_i}. \quad (15)$$

Here the total number of absorbing species is denoted by N . In the next sections we will show how both calibration models can be extended with this definition to investigate the effects of dyshemoglobins on the measurement.

2.3.1. Ratio-of-ratios

By adding the dyshemoglobins and using the relative concentrations χ , Eq. (7) can be expressed as:

$$R = \frac{\Delta A(\lambda_1)}{\Delta A(\lambda_2)} = \frac{\chi_{Hb} \epsilon_{Hb}(\lambda_1) + \chi_{HbO_2} \epsilon_{HbO_2}(\lambda_1) + \chi_{DysHb} \epsilon_{DysHb}(\lambda_1)}{\chi_{Hb} \epsilon_{Hb}(\lambda_2) + \chi_{HbO_2} \epsilon_{HbO_2}(\lambda_2) + \chi_{DysHb} \epsilon_{DysHb}(\lambda_2)}, \quad (16)$$

where similar to Eq. (7) the differences in ΔI s are expected to be negligible and these terms may therefore be dropped. When substituting this new expression of R into Eq. (9) and after re-arranging, one obtains:

$$SpO_2 = \frac{\chi_{HbO_2} + \chi_{Hb} \left(\frac{\epsilon_{Hb}(\lambda_1) \epsilon_{Hb}(\lambda_2) - \epsilon_{Hb}(\lambda_2) \epsilon_{Hb}(\lambda_1)}{\epsilon_{Hb}(\lambda_1) \epsilon_{HbO_2}(\lambda_2) - \epsilon_{Hb}(\lambda_2) \epsilon_{HbO_2}(\lambda_1)} \right) + \chi_{DysHb} \left(\frac{\epsilon_{Hb}(\lambda_1) \epsilon_{DysHb}(\lambda_2) - \epsilon_{Hb}(\lambda_2) \epsilon_{DysHb}(\lambda_1)}{\epsilon_{Hb}(\lambda_1) \epsilon_{HbO_2}(\lambda_2) - \epsilon_{Hb}(\lambda_2) \epsilon_{HbO_2}(\lambda_1)} \right)}{\chi_{HbO_2} + \chi_{Hb} \left(\frac{\epsilon_{HbO_2}(\lambda_2) \epsilon_{Hb}(\lambda_1) - \epsilon_{HbO_2}(\lambda_1) \epsilon_{Hb}(\lambda_2)}{\epsilon_{Hb}(\lambda_1) \epsilon_{HbO_2}(\lambda_2) - \epsilon_{Hb}(\lambda_2) \epsilon_{HbO_2}(\lambda_1)} \right) + \chi_{DysHb} \left(\frac{\epsilon_{DysHb}(\lambda_2) \epsilon_{Hb}(\lambda_1) - \epsilon_{DysHb}(\lambda_1) \epsilon_{Hb}(\lambda_2)}{\epsilon_{Hb}(\lambda_1) \epsilon_{HbO_2}(\lambda_2) - \epsilon_{Hb}(\lambda_2) \epsilon_{HbO_2}(\lambda_1)} \right)} \times 100\%, \quad (17)$$

which can be expressed in the form:

$$SpO_2 = \frac{\chi_{HbO_2} + \alpha \chi_{DysHb}}{\chi_{HbO_2} + \chi_{Hb} + \beta \chi_{DysHb}} \times 100\%. \quad (18)$$

The next step is to embed the definitions of *fractional* and *functional* SaO₂ into Eq. (18). These two SaO₂ definitions can be expressed in terms of the *relative* concentrations χ :

$$\begin{aligned} SaO_2^{fractional} &= 1 - \chi_{Hb} - \chi_{DysHb} \\ SaO_2^{functional} &= \frac{1 - \chi_{Hb} - \chi_{DysHb}}{1 - \chi_{DysHb}}. \end{aligned} \quad (19)$$

By substitution these expressions into Eq. (18), SpO₂ can be expressed as:

$$\begin{aligned} SpO_2 &= \frac{SaO_2^{fractional} + \alpha \chi_{DysHb}}{1 + (\beta - 1) \chi_{DysHb}} \times 100\% \\ SpO_2 &= \frac{SaO_2^{functional} (1 - \chi_{DysHb}) + \alpha \chi_{DysHb}}{1 + (\beta - 1) \chi_{DysHb}} \times 100\%. \end{aligned} \quad (20)$$

With these expressions we can investigate how the presence of dyshemoglobins in arterial blood influences the SpO₂ reading. Reported empirical results are obtained from pulse-oximeters with the common 660 and 940nm wavelength pair. To relate our theoretical model with the experimental observations, we evaluated Eq. (20) with these wavelengths. The results for different concentrations of the dyshemoglobins COHb and MetHb are visualized in Fig. 3.

From our simulation results visualized in Fig. 3 it can be observed that they agree with the experimental observations for both COHb and MetHb: for elevated levels of CO, SpO₂ is overestimated approximately proportional to the CO concentrations, whereas for elevated MetHb levels the SpO₂ reading becomes around 80% irrespectively of the true blood oxygenation level. Fig. 1 shows that at 660nm, MetHb looks much like (reduced) Hb. However, more importantly, at 940nm the extinction or absorbance of MetHb is markedly greater than that of either Hb or HbO₂. As a result, MetHb will contribute greatly to the perceived absorption of both these species, and will increase both the numerator and the denominator of the ratio of relative absorbances

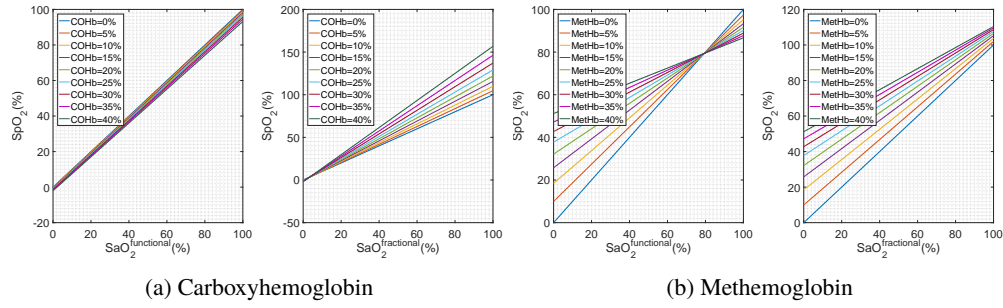


Fig. 3: Simulations on how the ratio-of-ratios based SpO_2 readings are affected for different concentrations of the dyshemoglobins (a) carboxyhemoglobin and (b) methemoglobin. The two wavelengths used are 660 and 940nm, which are commonly used in pulse-oximeters.

the oximeter calculates, driving this ratio towards 1, corresponding to an oxygenation level of around 80%. The absorption of COHb at 660nm is comparable to HbO_2 , whereas at 940nm the absorption is negligible. Therefore COHb “looks like” HbO_2 at 660nm and has essentially no effect on the 940nm infrared wavelength, leading to an overestimation of true oxygenation.

2.3.2. APBV

Similar to the ratio-of-ratios based method, the calibration model of the APBV method can also be extended in order to investigate the effects of dyshemoglobins on the SpO_2 reading. The presence of dyshemoglobins only affects the PPG term in Eq. (11), which with the introduction of relative concentrations can be expressed as:

$$PPG(\lambda) \approx \chi_{Hb} \epsilon_{Hb}(\lambda) + \chi_{HbO_2} \epsilon_{HbO_2}(\lambda) + \chi_{DysHb} \epsilon_{DysHb}(\lambda). \quad (21)$$

The pulse vector \vec{P}_{bv} can now be expressed as function of fractional SaO_2 and dyshemoglobin concentration χ_{DysHb} :

$$\vec{P}_{bv}(SaO_2^{fractional}, \chi_{DysHb}) = \begin{pmatrix} \frac{\int_{\lambda} I(\lambda) F^1(\lambda) C(\lambda) [SaO_2^{fractional} (\epsilon_{HbO_2} - \epsilon_{Hb}) + \chi_{DysHb} (\epsilon_{DysHb} - \epsilon_{Hb}) + \epsilon_{Hb}] d\lambda}{\int_{\lambda} I(\lambda) F^1(\lambda) C(\lambda) \rho_s(\lambda) d\lambda} \\ \frac{\int_{\lambda} I(\lambda) F^2(\lambda) C(\lambda) [SaO_2^{fractional} (\epsilon_{HbO_2} - \epsilon_{Hb}) + \chi_{DysHb} (\epsilon_{DysHb} - \epsilon_{Hb}) + \epsilon_{Hb}] d\lambda}{\int_{\lambda} I(\lambda) F^2(\lambda) C(\lambda) \rho_s(\lambda) d\lambda} \\ \vdots \\ \frac{\int_{\lambda} I(\lambda) F^N(\lambda) C(\lambda) [SaO_2^{fractional} (\epsilon_{HbO_2} - \epsilon_{Hb}) + \chi_{DysHb} (\epsilon_{DysHb} - \epsilon_{Hb}) + \epsilon_{Hb}] d\lambda}{\int_{\lambda} I(\lambda) F^N(\lambda) C(\lambda) \rho_s(\lambda) d\lambda} \end{pmatrix}, \quad (22)$$

and similar for functional SaO_2 :

$$\vec{P}_{bv}(SaO_2^{functional}, \chi_{DysHb}) = \begin{pmatrix} \frac{\int_{\lambda} I(\lambda) F^1(\lambda) C(\lambda) [SaO_2^{functional} (\epsilon_{HbO_2} + \epsilon_{Hb} (\chi_{DysHb} - 1)) + \chi_{DysHb} (\epsilon_{DysHb} - \epsilon_{Hb}) + \epsilon_{Hb}] d\lambda}{\int_{\lambda} I(\lambda) F^1(\lambda) C(\lambda) \rho_s(\lambda) d\lambda} \\ \frac{\int_{\lambda} I(\lambda) F^2(\lambda) C(\lambda) [SaO_2^{functional} (\epsilon_{HbO_2} + \epsilon_{Hb} (\chi_{DysHb} - 1)) + \chi_{DysHb} (\epsilon_{DysHb} - \epsilon_{Hb}) + \epsilon_{Hb}] d\lambda}{\int_{\lambda} I(\lambda) F^2(\lambda) C(\lambda) \rho_s(\lambda) d\lambda} \\ \vdots \\ \frac{\int_{\lambda} I(\lambda) F^N(\lambda) C(\lambda) [SaO_2^{functional} (\epsilon_{HbO_2} + \epsilon_{Hb} (\chi_{DysHb} - 1)) + \chi_{DysHb} (\epsilon_{DysHb} - \epsilon_{Hb}) + \epsilon_{Hb}] d\lambda}{\int_{\lambda} I(\lambda) F^N(\lambda) C(\lambda) \rho_s(\lambda) d\lambda} \end{pmatrix}. \quad (23)$$

As mentioned earlier the calibration of RR and APBV for a two wavelength system is identical, the SpO_2 determination procedure is however different. Instead of linking a ratio of amplitudes to an oxygenation level (1-D to 1-D mapping), with APBV a sweep over possible SpO_2 values is performed where the SpO_2 -dependent pulse vector which provides the pulse signal with the highest SNR is selected (N -D to 1-D mapping). Although dependent on the type of distortion,

in general the vector which has the minimum distance in L2-sense between the data and the examined pulse vector will be selected. When blood oxygenation levels within the range 0 – 100% with a sampling resolution of 0.1% are evaluated, the error of the SpO₂ reading for different CO-levels is visualized in Fig. 4a. The resulting errors for different levels of methemoglobin are visualized in Fig. 4b. When comparing the results from RR and APBV, it can be observed that the dyshemoglobins have a similar effect on both methods. However, since APBV typically only examines oxygenation levels within the range 0 – 100%, the resulting error can be biased, e.g. for CO.

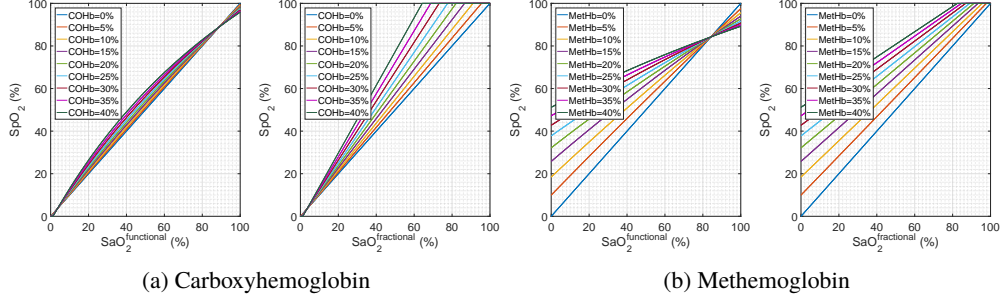


Fig. 4: Simulations on how the APBV-based SpO₂ readings are affected for different concentrations of the dyshemoglobins (a) carboxyhemoglobin and (b) methemoglobin. The two wavelengths used are 660 and 940nm, which are commonly used in pulse-oximeters. Although in large agreements with Fig. 3, there are differences observable because of the different selection criterium and restricted search area.

2.4. Wavelength selection

In the previous paragraphs we introduced the SpO₂ calibration models for both RR and APBV, and extended these to investigate how the presence of hemoglobins affects the measurement for the common 660 and 940nm wavelength pair used in pulse-oximeters. In this paragraph, we investigate how we can select the best wavelengths for three-wavelength camera-based pulse-oximetry for different optimization criteria.

2.4.1. Motion and SpO₂ contrast

To suppress motion artifacts in the PPG waveforms we profit from the fact that motion-induced intensity variations have a different mixture compared to the cardiac-induced intensity variations. The cardiac-induced mixture is compiled in the pulse vector \vec{P}_{bv} and is a function of SaO₂, whereas the motion is equally present in all wavelengths and can therefore be represented as the ‘motion’ vector $[1, \dots, 1]^T$ with shorthand notation $\vec{\mathbf{1}}$. The larger the discrepancy between both vectors, the better distortions can be suppressed enabling reliable measurements. Motion robustness can therefore be assessed by computing the angle between \vec{P}_{bv} and $\vec{\mathbf{1}}$:

$$\angle Motion = \left(\sum_{SaO_2 \in SaO_2} \text{acos} \left(\frac{\vec{P}_{bv}(SaO_2) \cdot \vec{\mathbf{1}}}{|\vec{P}_{bv}(SaO_2)| \cdot |\vec{\mathbf{1}}|} \right) \right) / S_0, \quad (24)$$

where S_0 denotes the number of evaluated oxygenation levels. We showed earlier that when adding a ‘redundant’ third wavelength this angle is never equal to zero, enabling distinction between the pulse signal and motion over the entire range of oxygenation levels.

Besides the criterion of motion robustness, another important criterion is the SpO₂ contrast; the change in pulse amplitudes as function of oxygenation level. A large contrast allows to detect

small variations in oxygenation levels and is therefore desirable. To assess the contrast, we compute the angle between the pulse vector at 0% and at 100% oxygenation:

$$\angle SpO_2^{contrast} = \arccos\left(\frac{\vec{P}_{bv}(SaO_2 = 0\%) \cdot \vec{P}_{bv}(SaO_2 = 100\%)}{|\vec{P}_{bv}(SaO_2 = 0\%)| \cdot |\vec{P}_{bv}(SaO_2 = 100\%)|}\right). \quad (25)$$

The results on the optimal wavelength selection for both criteria are presented in Sec. 3.1.1.

2.4.2. Dyshemoglobins

As shown in the previous paragraphs the presence of dyshemoglobins in arterial blood can have a large impact on the SpO₂ reading, leading to either false alarms or undetected clinically hazardous situations. Although its effects cannot be completely eliminated, it can be greatly reduced by a proper selection of wavelengths since not all wavelengths are equally affected. To determine the wavelength selection, we assess the effect of both dyshemoglobins on the reading by calculating the discrepancy between SaO₂ and SpO₂ values using our developed opto-physiological models. The results of this analysis are presented in Sec. 3.1.2.

2.4.3. Combined

In the previous paragraphs we elaborated on how to determine the optimal wavelengths for different criteria. In practise one has to select the wavelengths based on a weighted combination of the criteria. We therefore create an objective function including these criteria, each with an individual (positive) weighting constant:

$$\{\lambda_1^*, \lambda_2^*, \lambda_3^*\} = \underset{\lambda_1, \lambda_2, \lambda_3 \in \lambda | \lambda_1 < \lambda_2 < \lambda_3}{\operatorname{argmax}} \quad \alpha F^{SpO_2^{contrast}} + \beta F^{motion} + \gamma F^{DysHb} + \delta F^{P_{bv}^{contrast}}. \quad (26)$$

The values of the weighting constants can be set arbitrarily, depending on the requirements. The values of the individual objective functions are normalized in the range [0,1]. To prevent a cluttering of wavelengths, we included a fourth objective function, $F^{P_{bv}^{contrast}}$, which describes the variation *between* the elements in the vector to ensure a spread of the wavelengths. The results of the full-search optimization are presented in Sec. 3.1.3.

2.5. Detection of presence dyshemoglobins

As mentioned before, a dual-wavelength system cannot discriminate between more than two species. Although we used a three-wavelength system [3] before to improve robustness, we calibrated the system for the presence of Hb and HbO₂ only. The presence of dyshemoglobins would therefore lead to falsely-low or falsely-high SpO₂ readings. However, using three instead of two wavelengths does allow to design a reliability indicator for the SpO₂ measurement based on the various wavelength-pairs which are differently affected by the dyshemoglobins. We therefore create an index, ζ , which is equal to zero when there are no dyshemoglobins present in the blood and gives higher values when the measurement is likely inaccurate due to the presence of dyshemoglobins. Based on our calibration model, Eq. (11), we determine the amplitudes as function of oxygenation level for the three possible wavelength-pairs and the combined three-wavelengths:

$$\vec{P}_{bv}^1(SaO_2) = \left\| \begin{bmatrix} \left(\frac{AC}{DC}\right)_{\lambda_1} \\ \left(\frac{AC}{DC}\right)_{\lambda_2} \\ \left(\frac{AC}{DC}\right)_{\lambda_3} \end{bmatrix} \right\|, \quad \vec{P}_{bv}^2(SaO_2) = \left\| \begin{bmatrix} \left(\frac{AC}{DC}\right)_{\lambda_1} \\ \left(\frac{AC}{DC}\right)_{\lambda_2} \end{bmatrix} \right\|,$$

$$P_{bv}^3(SaO_2) = \left\| \left[\begin{array}{c} (\frac{AC}{DC})_{\lambda_1} \\ (\frac{AC}{DC})_{\lambda_2} \\ (\frac{AC}{DC})_{\lambda_3} \end{array} \right] \right\|, \quad P_{bv}^4(SaO_2) = \left\| \left[\begin{array}{c} (\frac{AC}{DC})_{\lambda_2} \\ (\frac{AC}{DC})_{\lambda_3} \end{array} \right] \right\|,$$

and use these to extract the four cardiac pulse signals \vec{S} :

$$\vec{S}^i = \vec{W}^i \mathbf{C}_n^i = k P_{bv}^i(SaO_2) [\mathbf{C}_n^i \mathbf{C}_n^{iT}]^{-1} \mathbf{C}_n^i \quad \text{for } i=1,2,3,4. \quad (27)$$

By selecting the pulse signals with the highest SNR, four individual SpO₂ estimates are obtained:

$$S_{max}^i = \underset{1 \leq j \leq N}{\operatorname{argmax}} \mathcal{F}(\vec{S}^i) \odot \mathcal{F}(\vec{S}^i)^* \quad \text{for } i=1,2,3,4 \quad (28)$$

These SpO₂ estimates will be equal for nominal dyshemoglobin concentrations, but will differ when these concentrations are elevated. We therefore propose to create a reliability index, ζ , which is defined as the standard deviation of the four estimates:

$$\zeta = \sigma(S_{max}^1, S_{max}^2, S_{max}^3, S_{max}^4). \quad (29)$$

The value of ζ is therefore proportional to the uncertainty of the SpO₂ measurement, which is very important for the clinical interpretation of the reading. It can be observed that the idea of using wavelength-pairs is not restricted to three wavelengths, but can be further extended to an arbitrary $N > 3$.

2.6. Measurement of dyshemoglobins

The calibration model used to design the reliability index ζ is similar to the one presented in our previous publication [3]. We showed earlier that by extending this model we can also predict how the presence of dyshemoglobins affects the wavelengths. We will now demonstrate that based on this extended calibration model we can not only detect, but also quantify the presence of dyshemoglobins in arterial blood. Instead of performing a sweep over oxygenation levels only, we now perform a search over both oxygenation levels *and* dyshemoglobin concentrations:

$$P_{bv}^1(SaO_2, \chi_{DysHb}) = \left\| \left[\begin{array}{c} (\frac{AC}{DC})_{\lambda_1} \\ (\frac{AC}{DC})_{\lambda_2} \\ (\frac{AC}{DC})_{\lambda_3} \end{array} \right] \right\|, \quad P_{bv}^3(SaO_2, \chi_{DysHb}) = \left\| \left[\begin{array}{c} (\frac{AC}{DC})_{\lambda_1} \\ (\frac{AC}{DC})_{\lambda_3} \end{array} \right] \right\|,$$

$$P_{bv}^2(SaO_2, \chi_{DysHb}) = \left\| \left[\begin{array}{c} (\frac{AC}{DC})_{\lambda_1} \\ (\frac{AC}{DC})_{\lambda_2} \end{array} \right] \right\|, \quad P_{bv}^4(SaO_2, \chi_{DysHb}) = \left\| \left[\begin{array}{c} (\frac{AC}{DC})_{\lambda_2} \\ (\frac{AC}{DC})_{\lambda_3} \end{array} \right] \right\|,$$

$$\vec{S}^i = \vec{W}^i \mathbf{C}_n^i = k P_{bv}^i(SaO_2, \chi_{DysHb}) [\mathbf{C}_n^i \mathbf{C}_n^{iT}]^{-1} \mathbf{C}_n^i \quad \text{for } i=1,2,3,4 \quad (30)$$

$$S_{max}^i = \underset{1 \leq j \leq N}{\operatorname{argmax}} \mathcal{F}(\vec{S}^i) \odot \mathcal{F}(\vec{S}^i)^* \quad \text{for } i=1,2,3,4 \quad (31)$$

$$(SpO_2, \hat{\chi}_{DysHb}) = \underset{SaO_2 \in \mathbf{SaO}_2, \chi_{DysHb} \in \chi_{DysHb}}{\operatorname{argmin}} \frac{e^{\sigma(S_{max}^1, S_{max}^2, S_{max}^3, S_{max}^4)}}{\mu(SNR(\vec{S}^1), SNR(\vec{S}^2), SNR(\vec{S}^3), SNR(\vec{S}^4))}, \quad (32)$$

where μ denotes the sample mean operator. In addition to the SNR-based selection criterion used for SpO₂, we also include the distribution of the optima in the selection criterion since the optima for the wavelength combinations coincide when the examined parameter setting matches the data. An illustration of the principle based on synthetic PPG data is visualized in Fig. 5. Here the oxygenation level is set at 95% and the dyshemoglobin concentration is set at 5%. By performing a sweep over both oxygenation levels and dyshemoglobin concentrations, SpO₂ and χ_{dys} can be determined simultaneously based on the distribution of the optima and SNR values.

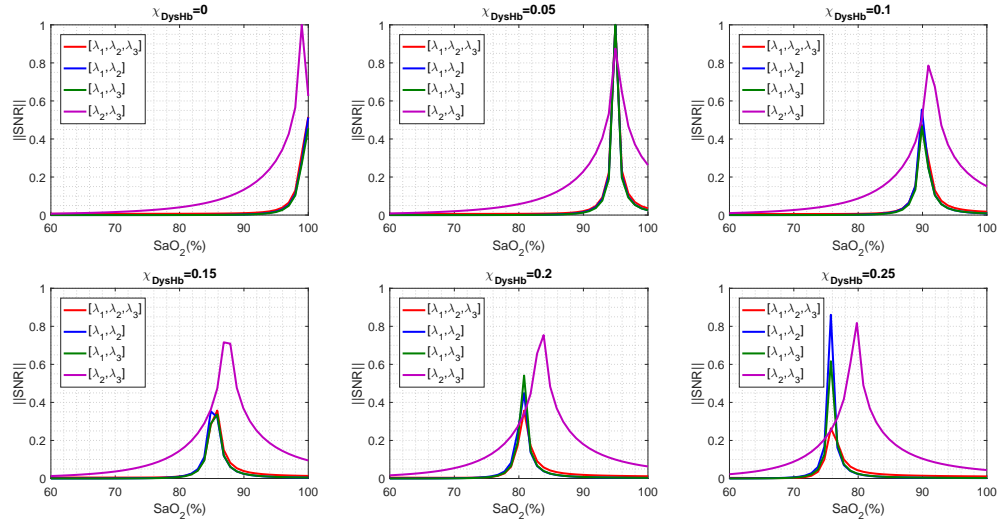


Fig. 5: Illustration of the simultaneous SpO₂ and dyshemoglobin concentration measurement principle based on synthetic PPG data, with the oxygenation level set at 95% and the dyshemoglobin concentration set at 5%.

The idea of using various wavelength-pairs to allow simultaneous SpO₂ and dyshemoglobin concentration measurements is not restricted to the ‘inverted’ APBV method, but could also be applied to the conventional RR approach. To verify the performance of both methods we used our calibration model to generate PPG signals with a CO-level of 10% and added multiplicative Gaussian noise with different amplitudes to the PPG waveforms. The results of this analysis are presented in Sec. 3.2.

Illustrative study

To verify the performance on real PPG data extracted from video recordings, we additionally created a dataset including heavy smokers because of their high suspicion of elevated CO-levels. A necessary consensus, given the variability level of COHb due to environmental CO, suggests an absolute upper limit of normal COHb of 3% for non-smokers and 10% for heavy smokers [18]. The setup for creating this dataset is similar to the one used for our earlier publication [3]. The study has been approved by the Internal Committee Biomedical Experiments of Philips Research and informed consent has been obtained from each subject. We asked all subjects to sit on a chair with their face focussed towards the cameras and remain static for the duration of 5 minutes. As reference we used a conventional SpO₂ finger probe connected to a Philips IntelliVue X2 patient monitor. Blood gas concentrations could unfortunately not be measured because of the unavailability of a blood gas analyzer or similar. We would therefore like to classify our results as illustration of the method. However, because of the non-smoking versus heavy smokers group,

a clear distinction in estimated CO-levels should be observable. The results of the study are presented in Sec. 3.2.

3. Results

3.1. Wavelength selection

To identify the optimal wavelengths for the optimization criteria discussed in Sec. 2.4, we perform a full-search within the wavelength-range 600 – 950 nm for a three-wavelength system where $\lambda_1 < \lambda_2 < \lambda_3$. Wavelengths $> 950\text{nm}$ are not included because of water absorption, whereby skin hydration levels start to play a role in the SpO_2 calibration.

3.1.1. Motion and SpO_2 contrast

The results of the wavelength search for both criteria are visualized in Fig. 6, where $\lambda_2 = \frac{\lambda_1 + \lambda_3}{2}$ and the sampling resolution is 2 nm. It can be observed that for motion robustness it is desirable to select the shortest wavelength, λ_1 , close to 600 nm. The selection of the longest wavelength, λ_3 , is less critical; from 800 nm onwards only small variations in motion robustness can be observed for all λ_1 . For SpO_2 contrast the wavelengths typically used in pulse-oximeters, 660 and 940nm, provide the best results. Because of the oxygenation-dependent pulse vector \vec{P}_{bv} , motion robustness is also a function of SpO_2 . To investigate this effect, instead of averaging over all oxygenation levels as we did before, we performed the search for oxygenation levels of 80, 90 and 100%. The results are visualized in Fig. 7. It can be observed that for the wavelengths which provide the largest SpO_2 contrast, motion robustness reduces for decreasing oxygenation levels, which was to be expected based on the absorption spectra of Hb and HbO_2 .

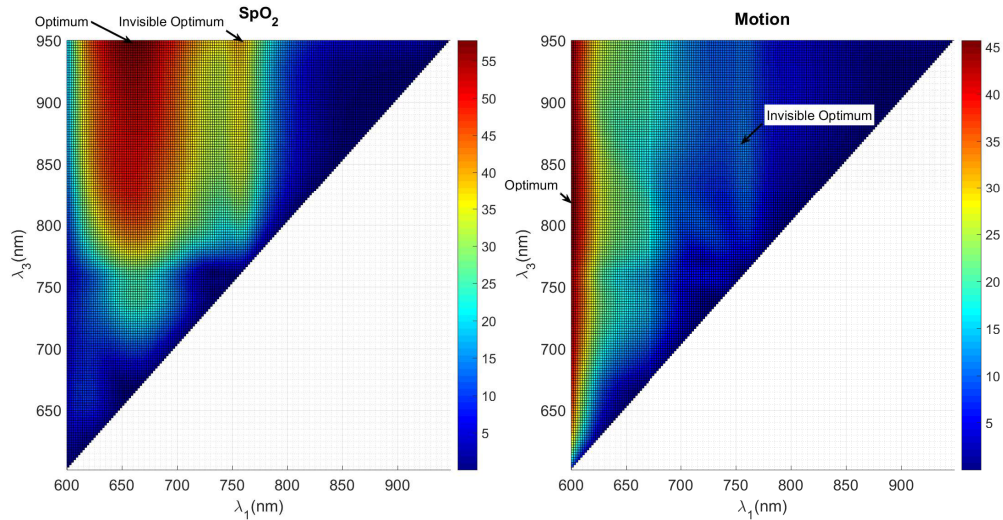


Fig. 6: The results of the wavelengths search for (left) SpO_2 contrast, and (right) motion robustness. The displayed values represent the angle (in degrees) between the pulse vector at 0% and 100% SpO_2 (left), and the angle between the pulse and motion vector (right).

3.1.2. Dyshemoglobins

The results of these simulations are visualized in Fig. 8a and Fig. 8b, respectively. For COHb, the effect on the SpO_2 reading can be vastly reduced when selecting the shortest wavelength λ_1 to be larger than 700nm. This result was to be expected since the absorption of COHb is strictly

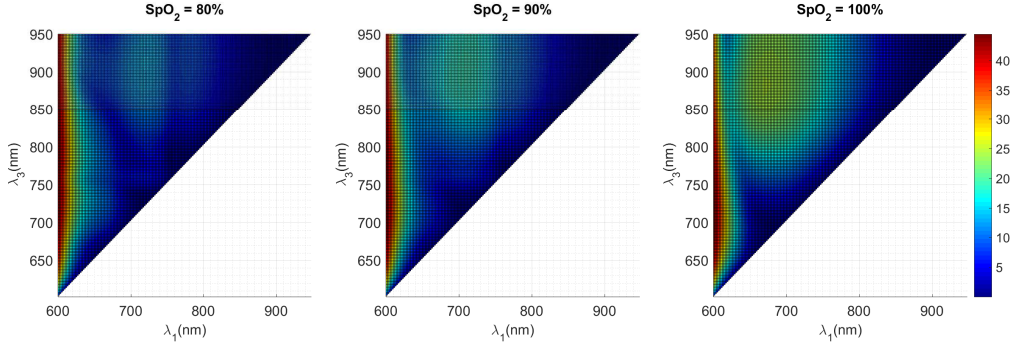


Fig. 7: Motion robustness is a function of the blood oxygenation level. We therefore investigated the robustness for 80, 90 and 100% SpO₂. It can be observed that within this range motion robustness reduces for decreasing oxygenation levels.

decreasing in the range 600-1000nm. For MetHb, it is preferred to select all wavelengths within the range $700 < \lambda < 800\text{nm}$, although the effect on the measurement cannot be reduced as much as for COHb.

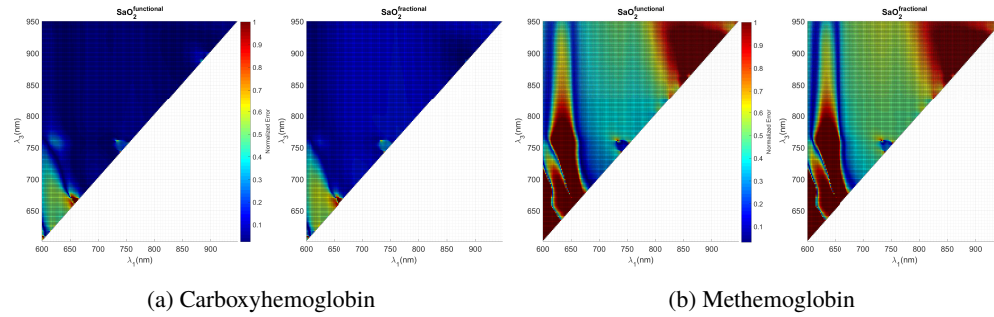


Fig. 8: Normalized error for COHb (a) and MetHb (b) when SpO₂ is calibrated for functional SaO₂ (left) and fractional SaO₂ (right). The error is calculated for a three wavelengths system with the middle wavelength linearly interpolated between the first and third wavelength.

3.1.3. Combined

In Fig. 9 we visualize the results when all weights are set equally and $\lambda_2 = \frac{\lambda_1 + \lambda_3}{2}$. The results for the full-search optimization are displayed in Tab. 1. For visualization we also performed the search with $\lambda_2 = \frac{\lambda_1 + \lambda_3}{2}$ and with a sampling resolution of 2 nm. The results of this search are visualized in Fig. 9. Although there are differences in optima between both dyshemoglobins, in general the highest scores are obtained for wavelengths which are widespread within the evaluated spectrum. When adding the constraint of invisibility to the human eye, the shortest wavelength shifts to 700nm for both dyshemoglobins.

3.2. Measurement of dyshemoglobins

The results obtained on synthetic PPG data are displayed in Table 2. We compared the performance of the original APBV method [3] (APBV^{3, λ}) with the proposed extended APBV method (APBV^{DysHb}) and the RR-based method (RR^{DysHb}) to simultaneously estimate SpO₂ and dyshemoglobin levels. For this experiment, the CO-level is set at 10% and the noise levels

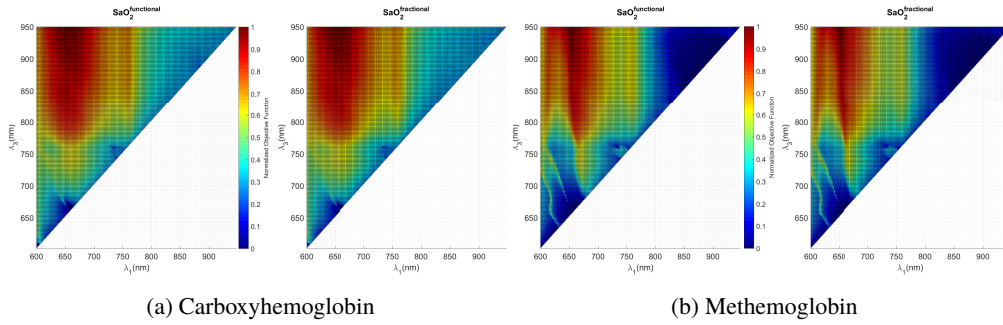


Fig. 9: Results of the combined objective function with equal weights and $\lambda_2 = \frac{\lambda_1 + \lambda_3}{2}$.

Table 1: Results from the full-search for a combination of objective functions. Allowing only invisible NIR wavelengths shifts the shortest wavelength to 700nm. The corresponding objective value reduction is denoted with Δ .

	$SaO_2^{functional}$						$\Delta(\%)$	$SaO_2^{fractional}$						$\Delta(\%)$
	[600-950]nm			[700-950]nm				[600-950]nm			[700-950]nm			
Dyshemoglobin	λ_1	λ_2	λ_3	λ_1	λ_2	λ_3		λ_1	λ_2	λ_3	λ_1	λ_2	λ_3	
COHb	655	805	950	700	805	950	-21.7	655	805	950	700	805	950	-20.5
MetHb	650	805	950	700	805	950	-31.1	650	805	950	700	805	950	-35.6

Table 2: Results of the extended RR and APBV methods to simultaneously measure SpO_2 and the dyshemoglobin concentration. The results are obtained on synthetic PPG data with a CO-level of 10%.

Noise level	APBV ^{3,λ}		APBV ^{DysHb}				RR ^{DysHb}			
	E_{SpO_2}	B_{SpO_2}	E_{SpO_2}	B_{SpO_2}	$E_{\chi_{DysHb}}$	$B_{\chi_{DysHb}}$	E_{SpO_2}	B_{SpO_2}	$E_{\chi_{DysHb}}$	$B_{\chi_{DysHb}}$
0	9.15	9.15	3.62e-1	1.97e-1	7.21e-1	-2.45e-1	5.10e-1	3.40e-2	9.46e-1	-3.40e-2
1e-3	9.12	9.12	4.49e-1	-2.31e-1	8.10e-1	3.88e-1	2.59e-1	-5.44e-2	5.71e-1	1.91e-1
1e-2	9.17	9.14	2.52e-1	-7.48e-2	4.22e-1	1.77e-1	6.26e-1	1.36e-2	9.46e-1	4.76e-2
1e-1	9.27	9.27	2.18e-1	1.09e-1	5.71	-3.40e-1	3.74	-2.36	7.56	5.53
1e0	9.33	9.33	8.37e-1	5.10e-1	1.44	-5.58e-1	16.6	-7.014	14.9	14.4
1e1	9.37	9.37	2.59	8.16e-1	4.31	-7.35e-1	26.8	-6.93	15.0	15.0

are expressed relative to the PPG amplitude. The errors and biases are indicated with E and B, respectively. The results show that for low noise levels, the performance of RR^{DysHb} is comparable to that of APBV^{DysHb}. However, as expected, when noise levels are high RR^{DysHb} renders inaccurate whereas APBV^{DysHb} still provides reliable measurements because of its ability to suppress distortions. As shown already mentioned in the previous section and verified by this experiment, APBV^{3,λ} overestimates SpO_2 approximately equal to the CO concentration.

So far, we illustrated the working principle of the proposed method based on synthetic PPG data. The results of the illustrative study are displayed in Table 3. It can be observed that there is a significant ($p < 0.05$) difference between the estimated CO-levels of the smokers (S) compared to the non-smokers (N-S), which is most noticeable for subject III. The average pulse-oximeter reading for this subject is 102%, with outliers up to more than 103%, which agrees with the overestimation of SpO_2 in the presence of elevated CO. It can also be observed that the results of APBV for both wavelength combinations is consistent, whereas RR shows large variations in results, which are likely caused by the low pulsatile amplitude of the 660 nm waveform. It should be noted that this subsection contains an illustrative example, and actual clinical validation is beyond the scope of this work.

Table 3: Results obtained on the smokers (S) versus non-smokers (N-S) dataset.

Subject	N-S/S	SpO ₂ ^{ref}	[660-800-840]nm					[760-800-840]nm				
			APBV ^{3,λ}		APBV ^{DysHb}		RR ^{DysHb}	APBV ^{3,λ}		APBV ^{DysHb}		RR ^{DysHb}
			SpO ₂	SpO ₂	χ _{COHb}	SpO ₂	χ _{COHb}	SpO ₂	SpO ₂	χ _{COHb}	SpO ₂	χ _{COHb}
I	N-S	98.1	98.6	98.3	1.26	97.8	1.59	97.8	97.2	1.33	97.4	1.12
II		95.6	96.1	95.2	0.87	94.2	2.87	95.9	95.4	0.67	95.2	0.89
III	S	102	103	95.2	8.46	99.3	0.97	102	95.4	8.22	94.1	8.97
IV		98.5	99.4	95.8	3.95	97.8	1.39	98.9	95.7	4.08	95.2	4.32

4. Discussion

The results obtained on smokers showed that elevated CO levels can be detected. During the analysis we assumed COHb to be the only dyshemoglobin present in arterial blood. We are aware that this assumption may not be valid in clinical practice, where other confounding factors may influence the measurement as well, among others the ones mentioned in this paper. We would also like to emphasize that all results are obtained on healthy patients with normal oxygenation levels. To claim clinical validity of the method an extensive dataset with large variations in both oxygenation levels and dyshemoglobin concentrations has to be created. This requires ground-truth measurement involving arterial blood samples.

The calibration models are based on the Beer-Lambert law and neglects the effects of scattering. Additionally, further assumptions have been made, e.g. that the skin is homogeneous and that the path length differences Δl for the various wavelengths are expected to be equal. This last assumption holds when the wavelengths are closely spaced in the range of evaluated wavelengths, but renders invalid when the wavelengths are widespread, introducing inaccuracies to the calibration. For the selected wavelengths used in this study we observed that the calibration model is fairly accurate, likely because of the close spacing of the wavelengths. We could however only verify the accuracy of the model for physiological conditions within a rather narrow range.

The main focus of our study was to identify when a SpO₂ measurement is unreliable or corrupted due to elevated dyshemoglobin concentrations, and the illustrative quantification of it can be considered a ‘bycatch’. The field of CO-oximetry specifically focusses on the quantification of these blood gases. To improve sensitivity of the quantification, a different selection of wavelengths compared to ours for COHb measurements is recommended since the absorption in NIR is rather low compared to the absorption for wavelengths in the range $500 < \lambda < 600\text{nm}$. Because of our desire to measure physiological parameters in (near)-darkness and the absence of a proper ground-truth, we identify the optimal wavelength selection for CO-oximetry out-of-scope for this study.

Besides the error sources listed in Sec. 2.1, fetal hemoglobin (HbF) is often identified to give inaccurate readings. Fetal Hb is the main oxygen transport protein in the human fetus during the last seven months of development in the uterus and persists in the newborn until roughly 6 months old. Functionally, HbF differs most from adult Hb (HbA) in that it is able to bind oxygen with greater affinity than the adult form, giving the developing fetus better access to oxygen from the mother’s bloodstream. This greater affinity to oxygen shifts the curve to the left. In newborns, HbF is nearly completely replaced by HbA by approximately 6 months postnatally, except in a few thalassemia cases in which there may be a delay in cessation of HbF production until 35 years of age. Zijlstra *et al.* measured the absorption spectra of both fetal and adult hemoglobin [19]. Based on these spectra we calculated the calibration curves and computed the differences between both as most pulse-oximeters are calibrated for adults only. The results of the comparison are visualized in Fig. 10 for the range 60 – 100% SpO₂. The worst-case error is approximately 2 percent, which is well-within the ISO requirement (ISO 80601-2-61, 2011, section 201.12.1.101.2.2) of an error < 4%. This confirms the earlier results obtained on actual neonatal data that showed that there is no clinically significant effect on pulse oximetry [20].

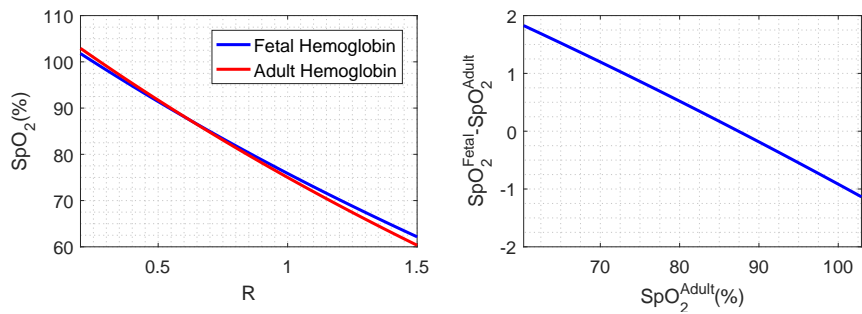


Fig. 10: Comparison between the calibration curves of fetal and adult hemoglobin (left) and the corresponding error (right).

The misconception that HbF does have an influence on the SpO₂ reading is likely caused by the effect it has on CO-oximeter readings, where HbF may be misread as COHb thereby spuriously lowering the reading [21].

5. Conclusion

We have identified possible confounding factors in camera-based pulse-oximetry and showed how a proper wavelength selection based on developed opto-physiological models could reduce the impact of some of these factors on the measurement. This investigation leads to wavelength recommendations for individual criteria together with a combined optimization criterion. Based on our earlier presented method for robust SpO₂ measurements using ‘priors’ of oxygenation levels, we proposed to create wavelength-pairs from the three-wavelength system, allowing the formulation of a reliability index of the measurement, which is important for the clinical interpretation. Finally, we showed that by performing a search over both oxygenation levels and dyshemoglobin concentrations, dyshemoglobins can not only be detected but also quantified. We think this study presents important design considerations to the relatively novel field of camera-based pulse-oximetry. Furthermore, based on preliminary results, we showed that the extension to camera-based pulse CO-oximetry seems feasible.

Funding

This research was performed within the framework of the IMPULS-II program for the Data Science Flagship project.

Acknowledgement

The authors would like to thank B. Balmaekers of Philips Research for his valuable contributions to this paper. Furthermore, we would like to thank all volunteers who participated in the experiments.

Disclosures

The authors declare that there are no conflicts of interest related to this article.